Biogeosciences

Anthropogenic carbon distribution in the eastern South Pacific Ocean

C. Goyet[1], R. Ito Gonçalves[2], and F. Touratier[1]

[1]IMAGES, Université de Perpignan, 52 avenue Paul Alduy, 66860 Perpignan, France
[2]Instituto Oceanográfico, Universidade de São Paulo, Pça. do Oceanográfico, 191 Cidade Universitária, 05508-900
São Paulo-SP, Brasil

Abstract. We present results of the CO_2/carbonate system from the BIOSOPE cruise in the Eastern South Pacific Ocean, in an area not sampled previously. In particular, we present estimates of the anthropogenic carbon (C_{ant}^{TrOCA}) distribution in the upper 1000 m of this region using the TrOCA method. The highest concentrations of C_{ant}^{TrOCA} found around 13° S, 132° W and 32° S, 91° W, are higher than 80 μmol.kg^{-1} and 70 μmol.kg^{-1}, respectively. The lowest concentrations are observed below 800 m depth ($\leq 2 \, \mu$mol.kg^{-1}) and within the Oxygen Minimum Zone (OMZ), mainly around 140° W ($<11 \, \mu$mol.kg^{-1}). As a result of the anthropogenic carbon penetration there has been decrease in pH by over 0.1 on an average in the upper 200 m. This work further improves our understanding on the penetration of anthropogenic carbon in the Eastern Pacific Ocean.

1 Introduction

While the ocean is known to be globally a sink for anthropogenic CO_2, the equatorial belt is an upwelling area where some anthropogenic carbon can be re-injected into the atmosphere. Thus, the equatorial belt (from 10° N to 10° S) plays a significant role in the global carbon cycle (Le Borgne et al., 2002). It annually supplies approximately 0.7–1.5 Pg C as CO_2 gas to the atmosphere. It is the largest natural source of CO_2 from the ocean (Takahashi et al., 1997; Feely et al., 1999). As much as 72% of the CO_2 outgassing from the world's oceans can be attributed to the equatorial Pacific alone.

The South Pacific Ocean (from 10° S down to 60° S) is globally considered as a sink area for anthropogenic carbon (Chen, 1993), however there is a strong zonal variability. Indeed, the western equatorial zone is the largest oceanic source of CO_2 to the atmosphere, while the eastern equatorial Pacific is considered as CO_2 sink (Tans et al., 1990; Murray et al., 1992; Murray et al., 1995). Here we present results from the BIOSOPE (BIogeochemistry and Optics SOuth Pacific Experiment) cruise in the Eastern (East of 142° W) South Pacific Ocean along a $\sim$8000 km long transect (Fig. 1). This transect covered a variety of hydrodynamic and trophic properties from the extremely productive upwelling waters of the Chilean coast to the extremely oligotrophic waters of the central gyre of the South Pacific Ocean, a priori expected to be the least productive oceanic area of the world (Longhurst, 1998; Claustre et al., 2008).

Here, we use data from the BIOSOPE cruise to investigate the oceanic anthropogenic carbon distribution using the TrOCA method (Touratier and Goyet, 2004 a, b; Touratier et al., 2007). We then quantify its impact in term of ocean acidification taking also into account the hydrodynamic characteristics of the area.

2 Material and methods

2.1 Sampling

The BIOSOPE cruise onboard R/V ATALANTE, departed from Tahiti on 26th October 2004 and ended on 11th December 2004 at Conception (Chile). The cruise track went through the oligotrophic area in the central part of the South Pacific Gyre (SPG) along a transect starting from the Marquises Islands around 70° W, 8° S to the Chilean coast at 141° W, 35° S.
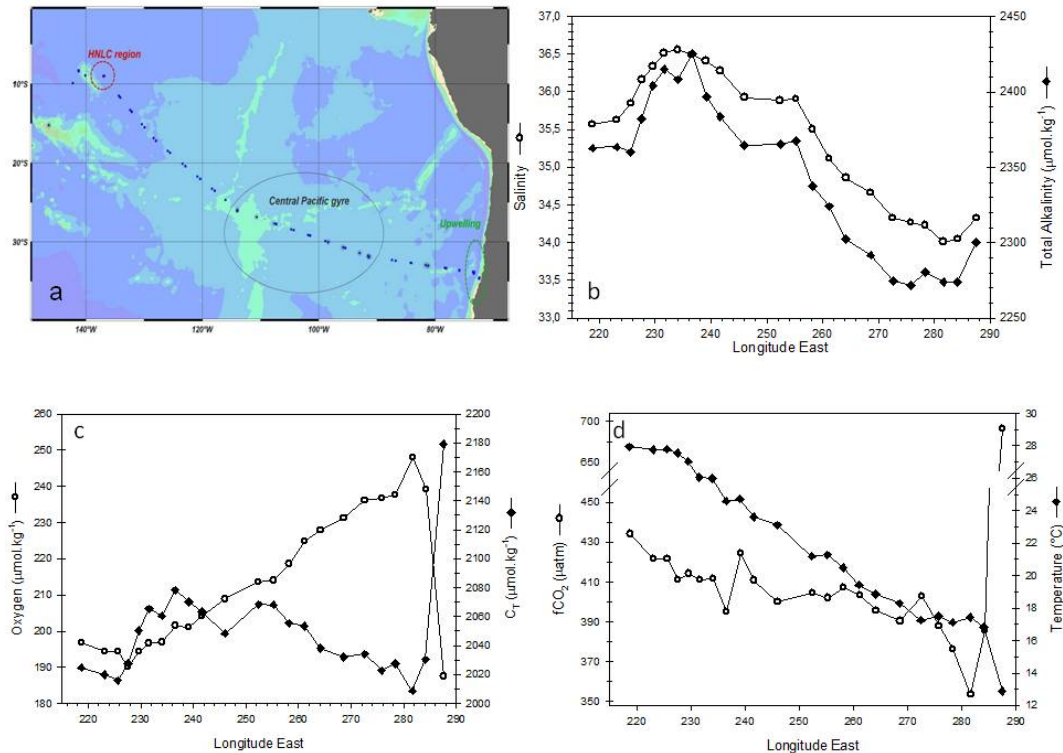
Fig. 1. Station locations of the 2004 BIOSOPE cruise **(a)**, and sea-surface properties; **(b)** salinity and total alkalinity, **(c)** Oxygen and Total CO_2, and **(d)** temperature and CO_2 fugacity.

Water sampling and measurements of temperature and salinity were made using a SeaBird SBE 911plus CTD/Carousel system fitted with an SBE 43 oxygen sensor. From the 223 vertical profiles, 23 were sampled for studying the oceanic carbon cycle (Fig. 1a). At each of these stations an average of 22 samples were collected in the upper water column from the near surface ($\sim$3 m depth) to $\sim$500 m depth. Only four of these stations were sampled down to the near bottom depth ($>$1000 m).

Seawater was sampled into 500ml borosilicate-glass bottles and poisoned with a saturated solution of mercuric chloride before being sealed. The samples were then stored and shipped back to the laboratory where the measurements were performed within a month after the end of the cruise.

2.2 Measurements of total dissolved inorganic carbon (C_T) and total alkalinity (A_T)

The measurements of total dissolved inorganic carbon (C_T) and total alkalinity (A_T) were performed by potentiometric acid titration in a closed cell (Edmond, 1970; DOE, 1994). From replicate analysis of reference seawater samples, (CRMs from Dr Andrew Dickson of Scripps Institution of Oceanography), both the precision and the accuracy of the analyses were determined to be within 1.5 μmol.kg^{-1} for C_T and 1.7 μmol.kg^{-1} for A_T.

3 Determination of anthropogenic carbon distribution

Since anthropogenic carbon in the ocean cannot be measured directly, it is calculated according to various models based upon different assumptions. Although, the early attempts to estimate the distribution of anthropogenic carbon in the ocean (Brewer, 1978; Chen and Millero, 1979) were criticized (Shiller, 1981; Broecker et al., 1985), they initiated a vigorous debate concerning the "best way" to determine the distribution of anthropogenic carbon in the ocean.

Since then, many different methods have been developed. Many are still based on the initial work of the late 70's with various improvements (e.g. ΔC^* approach of Gruber et al., 1996; Pérez et al., 2002; LM approach of Lo Monaco et al., 2005a; Vázquez-Rodríguez et al., 2009). Others are based upon completely new concepts such as water-mass mixing (Goyet et al. 1999); or similarity with CFCs or SF$_6$ penetration (e.g. Goyet and Brewer, 1993; TTD approach of Waugh et al., 2004; Waugh et al., 2006; Tanhua et al., 2008); or a new water-mass tracer "TrOCA" (Touratier and Goyet, 2004a, b; Touratier et al., 2007).

Many studies have been carried out and others are still underway to compare the results of these various methods (Coatanoan et al., 2001; Friis, 2007; Vázquez-Rodríguez et al., 2008). In the light of these previous results, here we have chosen to use the TrOCA approach (Eq. 1), which is the

simplest, and yet a very reliable method, to study the distribution of anthropogenic carbon in the Eastern Pacific Ocean.

As a very brief reminder, using the TrOCA approach (Touratier et al., 2007), the anthropogenic carbon concentration in seawater (C_{ant}^{TrOCA}) is calculated using the following relationship:

$$C_{ant}^{TrOCA}=$$

$$\frac{O_2+1.279\left[C_T-\frac{1}{2}A_T\right]-e^{\left(7.511-(1.087\times10^{-2})\theta-\frac{7.81\times10^5}{A_T^2}\right)}}{1.279} \quad (1)$$

4 Hydrography

In the upper 500 m, the study area is dominated by both the South Equatorial Current and the Peru Current. The region can be roughly separated into five main areas (Claustre et al., 2008): (1) the Sub Equatorial area (142° W–132° W) (near the Marquise Islands) that is influenced by the equatorial regime; (2) the transition zone (132° W–123° W) between the sub-Equatorial area and the South Pacific Gyre (SPG); (3) the central part of the SPG (123° W–101° W); (4) the transition zone between the SPG and the coastal upwelling area (100° W–81° W); and (5) the coastal upwelling area (East of 81° W).

Both the easterly winds which drive away the surface waters and the prevailing southerly winds off the Peruvian coast provoke an upwelling along the equator and the Peruvian coast. The cold and relatively low-salinity waters of the Humboldt Current are advected northward from Chile to off-shore of Peru (Strub et al., 1998; Kessler, 2006). These eastern boundary waters merge to supply the westward-flowing South Equatorial Current (SEC), which is subject to the divergence, north and south of the equator, and generates upwelling of subsurface waters having high salinity, C_T, and nutrient concentrations to the surface (Kessler, 2006). Since chlorophyll concentrations remain low and the macronutrients are not depleted, this region is a HNLC (high-nutrient/low-chlorophyll) area (Minas et al., 1986).

In the SEC (South Equatorial Current) the surface layer is characterized by the warm and high-salinity SubTropical Surface Water (STSW, $S>35$). Along the coast of South America, the Peru Current is characterized by cold, low-salinity water (Fiedler and Talley, 2006). Closer to the coast, the Gunther Undercurrent is located between 100 and 400 m depth, and is characterized by the Equatorial SubSurface Water (ESSW) with a relatively high salinity (34.7–34.9) and nutrients concentrations, low temperatures (~12.5° C) and dissolved oxygen (Shaffer et al., 1995; Blanco et al., 2002). Underneath the SEC, the Subtropical Underwater (ESPCW: Emery and Meincke, 1986; Tomczak and Gogfrey, 2001) is located between 110° W–150° W, and 10° S–20° S around 150 m depth. At a few hundred meters water depth (around 200–400 m), there are two oxygen minimum zones (OMZ)

which are driven by the degradation of organic matter sinking out of the euphotic zone and modified by ocean circulation (Wyrtki, 1962). The oxygen minimum zone is strongly linked with one of the most productive marine ecosystems in the world, so that the oxygen deficiency is attributable to the high biological productivity at the surface. The largest area of low oxygen in the world lies in the thermocline in the Eastern Tropical Pacific Ocean. The area of low oxygen extends as tongues to either side of the equator from Central and northern South America across the Eastern Tropical Pacific Ocean (see Fiedler and Talley, 2006).

At intermediate water depths, the Eastern South Pacific Intermediate Water (ESPIW: Schneider et al., 2003), properties are those of the Subantarctic Water; it is relatively cool (~12°C) and fresh ($S\sim34.25$) and it is bellow STSW offshore and above ESSW closer to the coast (Blanco et al., 2001). The influence of Antarctic Intermediate Water (AAIW) can be seen at depths of around 500 to 700 m, typically south of 26° S and with salinities <34.5 and temperatures <7°C (Blanco et al., 2001; Zenk et al., 2005; Fiedler and Talley, 2006). The bottom water originates from the Lower Circumpolar Water (LCPW).

The South Pacific subtropical gyre (SPSG) region (13–23° S, 80/87–140° W) has the highest surface (0–100 m) salinities (averaged $S=36.1$) of the Eastern Tropical South Pacific Ocean regions and is defined by the "subtropical surface water" of Fiedler and Talley (2006).

5 Results

5.1 Distribution of the CO_2/carbonate properties in the surface ocean along the cruise track

Figure 1b, c, d illustrates the sea-surface distribution of the measured temperature, salinity, total alkalinity, oxygen, and total CO_2, as well as the computed fCO_2 (sea-surface CO_2 fugacity) along the cruise track in the Eastern Tropical South Pacific Ocean. Figure 1b shows the clear (linear) relationship between sea-surface salinity and sea-surface total alkalinity. Within the central Pacific gyre, we observed a large A_T gradient (>100 μmol.kg^{-1}) associated with a salinity gradient of 2. Over the BIOSOPE cruise track, sea-surface A_T could be estimated from the sea-surface salinity with the relationship:

$$A_T = 58.40S + 275.70 \, \mu mol.kg^{-1} (r = 0.9831) \quad (2)$$

Note that this relationship holds even in the upwelling area, thus suggesting that A_T could be correlated with salinity well below the sea-surface layer.

Figure 1c illustrates the mirror effect of the oxygen and total CO_2 concentrations. As the oxygen concentrations rise, the total CO_2 decreases. This also holds throughout the water column as illustrated by the coastal upwelled waters. What is striking here, is the amplitude of geographical variation

of C_T. Except for the local coastal upwelling, the C_T variations are relatively small ($<80\,\mu\text{mol.kg}^{-1}$) compared with those of A_T ($>100\,\mu\text{mol.kg}^{-1}$) as mentioned above. This indicates that, as expected in an oligotrophic area, that in this region, the water properties are mainly controlled by the physical forcing.

These distributions unequivocally indicate that compared with the properties of the adjacent waters, the coastal upwelling brings relatively cold, high salinity, high A_T low O_2, and C_T rich water to the surface. Surface warming further decreases the solubility of CO_2 gas in sea water and enhance its CO_2 fugacity, thus favoring its venting to the atmosphere. The high wind then further facilitates the rate of transfer across the air-sea interface. This venting to the atmosphere is only reduced slightly by biological uptake of CO_2 by plankton. Furthermore, widespread iron limitation causes C_T (in addition to nitrate) to remain unused in the HNLC waters of the open ocean.

Figure 1d illustrates that in general as the temperature rises, the CO_2 fugacity rises. During the BIOSOPE cruise, except in the coastal upwelling area, sea-surface $f\text{CO}_2$ also rises with sea-surface to reach over $430\,\mu\text{atm}$ near the Marquise Islands. In the Peruvian coastal upwelling (PCU), the sea-surface temperature is relatively low since it comes from deeper layers, however this water is CO_2 rich (Fig. 1c), thus as it warms up in contact with the atmosphere, its $f\text{CO}_2$ rises quickly reaching up to $700\,\mu\text{atm}$ (Fig. 1d). Since $f\text{CO}_2$ in the atmosphere above this region of the Pacific Ocean was close to $376\,\mu\text{atm}\pm2\,\mu\text{atm}$ at the time of the cruise (2004), this ocean area was a significant source of CO_2 to the atmosphere.

5.2 Distributions of the CO_2/carbonates properties and their associated physical properties in the ocean section along the cruise track

Since most of the stations were sampled only down to 500 m-depth, and only three stations were sampled below 1000 m-depth, here we present (Fig. 2) the geographical distributions of the measured properties T, S, O_2, A_T, C_T and pH from the surface down to 1000 m-depth along the cruise track. However, the few data not shown here (below 1000 m-depth) are available through the BIOSOPE data base (http://www.obs-vlfr.fr/proof/vt/op/ec/biosope/bio.htm).

The highest T and S correspond to the water masses STSW at the surface and the Eastern South Pacific Central Waters (ESPCW) at $\sim$100 m (Fiedler, 2006). Low C_T concentrations ($<2100\,\mu\text{mol.kg}^{-1}$) also correspond to ESPCW and STSW (located between 100° W and 140° W longitudes within the upper 100 m depth).

In the eastern South Pacific Ocean the distributions of S, T, C_T, A_T, O_2, and pH (Fig. 2) reflect the influence of the Peru Current (Pennington et al., 2006). Not far from the Chilean coast (88° W) and around 500 m depth, elevated concentrations of C_T ($\geq2200\,\mu\text{mol.kg}^{-1}$) and low concen-

trations of A_T ($\leq2300\,\mu\text{mol.kg}^{-1}$) are observed in the dense ($\sigma\geq26$), cold and low salinity AAIW waters. In this area, C_T distribution follows a general pattern of a consistent increase with increasing depth down to 500 m. This corresponds to what was observed by Fiedler and Talley (2006) for nutrients and suggests the effects of biological uptake in surface waters and remineralization in deeper waters.

Since the C_T and O_2 profiles are mirror images of each other below the mixed layer depth (Goyet and Davis, 1997), the zones of highest C_T concentrations (Fig. 2) correspond to the OMZ (near the coast between 150m and 400 m-depth, and in the South Equatorial Current seen here around 140° W 10° S between 300 m and 600 m-depth), as described above.

In the oligotrophic area (130° W–110° W corresponding to the area between 2300 km and 6300 km), down to 300 m depth, both the pH and the O_2 concentrations are relatively high (>8 and $>200\,\mu\text{mol.kg}^{-1}$, respectively), while C_T is well below $2100\,\mu\text{mol.kg}^{-1}$.

5.3 Distributions of anthropogenic CO_2 concentrations and anthropogenic pH variations

The computed anthropogenic CO_2 ($C_{\text{ant}}^{\text{TrOCA}}$) distribution as well as its associated anthropogenic pH variations, from the surface down to 1000 m-depth are illustrated in Fig. 3.

Except for the shallow coastal areas, the highest $C_{\text{ant}}^{\text{TrOCA}}$ concentrations (close to $80\,\mu\text{mol.kg}^{-1}$), are observed around 13° S, 132° W. This ocean area is characterized by the ESPCW that is well ventilated. It is approximately 5 years old according to the tracer ages (Fiedler and Talley, 2006). Its origin is in the subduction region around 26° S, 110° W.

The water around 34° S, 76° W is characterized with relatively high anthropogenic CO_2 concentrations compared with the surrounding waters and it is thus particularly distinguished by high anthropogenic pH variations >0.1. Close to South America the anthropogenic CO_2 concentrations are controlled by the origin of the upwelling (especially its depth) and by the thermocline position. According to Carr and Kearns (2003), the upwelling water comes from isopycnal layers ranging from $\sigma_\theta=25.6\,\text{kg.m}^{-3}$ to $\sigma_\theta=26.2\,\text{kg.m}^{-3}$. Between 15° S and 34° S, the vertical displacement of the upwelled waters at the ocean surface does not typically exceed 50 m.

In general, the distribution of anthropogenic CO_2 (Fig. 3) shows that even in an area where the ocean is a CO_2 source for the atmosphere, at least the upper 400 m of the ocean is contaminated with anthropogenic CO_2. Furthermore, results from this highly oligotrophic area, indicate that even when biological activity is low and therefore does not draw down atmospheric CO_2, the upper ocean is affected by anthropogenic CO_2 carried by ocean circulation.

The lowest $C_{\text{ant}}^{\text{TrOCA}}$ concentrations are observed below 800 m and within the OMZ, especially around 140° W (near the Marquise Islands where $C_{\text{ant}}^{\text{TrOCA}}<15\,\mu\text{mol.kg}^{-1}$ between $\sigma_\theta=26.5\,\text{kg.m}^{-3}$ and $\sigma_\theta=27.0\,\text{kg.m}^{-3}$). Based upon the
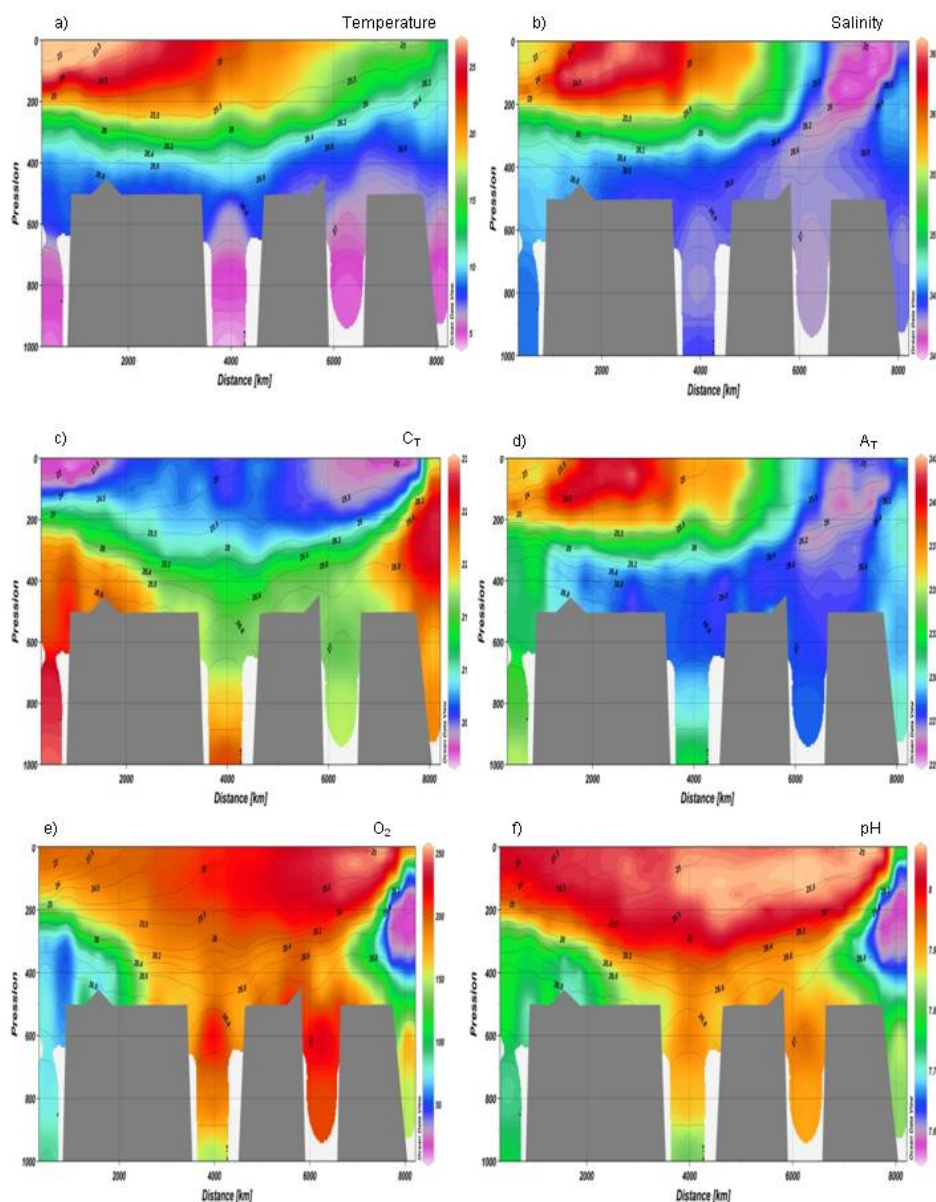
Fig. 2. Vertical distribution of the physicochemical parameters: **(a)** temperature (°C), **(b)** Salinity, **(c)** C_T (μmol.kg^{-1}), **(d)** A_T (μmol.kg^{-1}), **(e)** O_2 (μmol.kg^{-1}), **(f)** pH.

anthropogenic CO_2 concentrations and the observed sharp pycnocline within the subsurface water of the SEC, it can be inferred that ventilation is poorer in this OMZ (Fiedler and Talley, 2006) than in the OMZ of the Peru undercurrent.

Another area with a relatively low $C_{\mathrm{ant}}^{\mathrm{TrOCA}}$ penetration is around the longitudes between 100° W and 110° W in the 200 m–300 m depth range. This region is particularly well illustrated (Fig. 3b) with very low anthropogenic pH variations (<0.075). It represents the eastern part of the subduction of the Subtropical Underwater, and exhibits the deepest mixed layers.

The isoline $C_{\mathrm{ant}}^{\mathrm{TrOCA}}$=5 μmol.kg^{-1} indicates that anthropogenic CO_2 has already penetrated down to ~600 m depth at 141° W, 8° S and it penetrated even deeper down to ~1700 m at 130° W, 26° S. Close to the Chilean coast this isoline was located around 1100 m. In most parts of the area, this isoline was below the 27.1 kg.m^{-3} isopycnal. This indicates the presence of old waters.

5.4 Relationship between $C_{\mathrm{ant}}^{\mathrm{TrOCA}}$ and circulation

According to Chen (1993), in the Pacific Ocean, anthropogenic CO_2 doesn't penetrate below the main thermocline
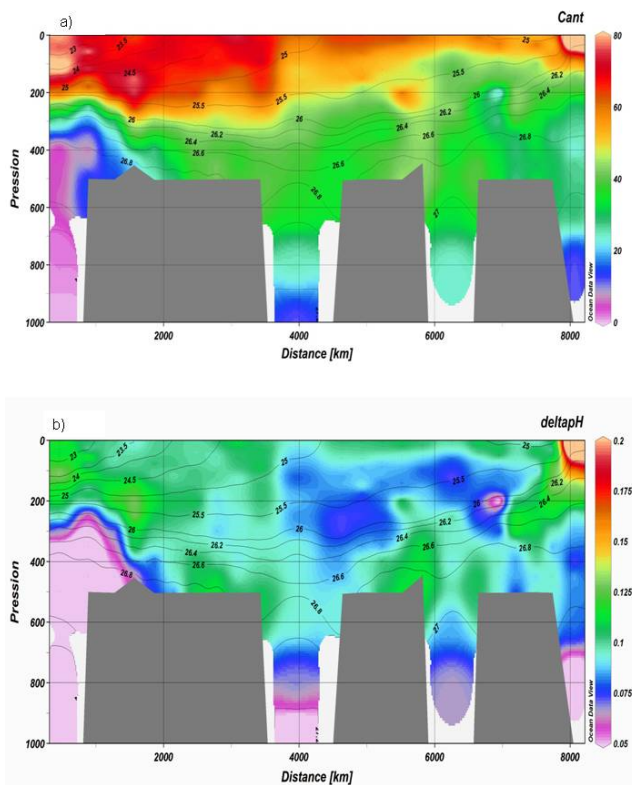
Fig. 3. Vertical distribution of **(a)** the calculated anthropogenic CO_2 ($C_{\mathrm{ant}}^{\mathrm{TrOCA}}$ μmol.kg^{-1}), and **(b)** the calculated anthropogenic pH variations.

because there is no deep water formation in the North Pacific Ocean. The shallowest penetration outside the Southern Ocean occurs in the eastern equatorial region where the anthropogenic CO_2 penetrates down to 400 m. This shallow penetration in the equatorial Pacific reflects water circulation with a high rate equatorial upwelling (Wyrtki, 1981; Broecker and Peng, 1998).

Shallow vertical penetration of $C_{\mathrm{ant}}^{\mathrm{TrOCA}}$ is generally observed in regions of upwelling. The isopycnal layers in the tropical thermocline tend to be shallow and thin, minimizing the movement of $C_{\mathrm{ANT}}^{\mathrm{TrOCA}}$ – laden waters into the ocean interior and limiting $C_{\mathrm{ant}}^{\mathrm{TrOCA}}$ rich waters to the upper layers.

The results presented here, show that the maximum depth of $C_{\mathrm{ant}}^{\mathrm{TrOCA}}$ penetration into the south-eastern Pacific (between 8° S and 35° S) is located at longitudes between 100° W and 130° W. This happens since westward of 130° W the intermediate waters are ventilated very slowly and these waters have very low $C_{\mathrm{ant}}^{\mathrm{TrOCA}}$ concentrations. Eastern of 100° W the ESPIW and the ESSW dominate the anthropogenic CO_2 distribution and prevent its deep penetration. As a consequence the acidification of the ocean area remains below the 0.13 pH level and is essentially concentrated in the upper 500 m-depth.

6   Conclusions

In summary, in spite of the high variability in the anthropogenic carbon distribution, due to the complex interactions between biogeochemical and hydrographic processes in the Eastern Pacific Ocean, this work illustrates that today anthropogenic carbon is present in the upper layers of the ocean at significant level even in oligotrophic areas and/or in CO_2 source areas for the atmosphere. Therefore, this study further demonstrates the importance of ocean circulation in storage (or outgassing) of anthropogenic CO_2 in the ocean. As the anthropogenic CO_2 penetrates into the ocean, the acidification of water especially of the upper ocean becomes significant and will in turn have a large impact on marine living organisms. Coupled with changes in ocean circulation due to global warming, these varying ocean properties should be further studied to better understand and predict their evolution.

References

Blanco, J. L., Thomas, A. C., Carr, M.-E., and Strub, P. T.: Seasonal climatology of hydrographic conditions in the upwelling region off northern Chile, J. Geophys. Res. Oceans, 106, 11451–11467, 2001.

Blanco, J. L., Carr, M.-E., Thomas, A. C., and Strub, P. T.: Hydrographic conditions off northern Chile during the 1996–1998 La Ninna and El Nino events, J. Geophys. Res., 107, 1–3, 2002.

Brewer, P. G.: Direct observations of the oceanic CO_2 increase, Geophys. Res. Lett. 5, 997–1000, 1978.

Brewer, P. G., Goyet, C., and Friederich, G.: Direct observation of the oceanic CO_2 increase revisited, Proceedings of the Nature Academia of Sciences, 94, 8308–8313, 1997.

Broecker, W. S. and Peng, T.-H.: Greenhouse Puzzles, 287 pp., 1998.

Broecker, W. S., Takahashi, T., and Peng T.-H.: Reconstruction of past atmospheric CO_2 from the chemistry of the contemporary ocean: An evaluation, Tech. Rep. TRO 20, US Dep. Of Energy, Washington D.C., 1985.

Carr, M.-E. and Kearns, E. J.: Production regimes in four Eastern Boundary Current systems, Deep Sea Res. Part II, Topical Studies in Oceanography, 50, 3199, 2003.

Chen, C.-T. A. and Millero, F. J.: Gradual increase of oceanic CO_2, Nature, 277, 205–206, 1979.

Chen, C.-T. A.: The oceanic anthropogenic CO_2 sink, Chemosphere, 27, 1041–1064, 1993.

Claustre, H., Sciandra, A., and Vaulot, D.: Introduction to the special section bio-optical and biogeochemical conditions in the South East Pacific in late 2004: the BIOSOPE program, Biogeosciences, 5, 679–691, 2008,
http://www.biogeosciences.net/5/679/2008/.

Coatanoan, C., Goyet, C., Gruber, N., Sabine, C. L., and Warner, M.: Comparaison of two approaches to quantify anthropogenic CO_2 in the ocean: Results from the northern Indian Ocean, Global Biogeochem. Cy., 15, 11–25, 2001.

DOE: Hanbook of methods for the analysis of the various parameters of the carbon dioxide system in seawater, version 2, in: ORNL/CDIAC-74., edited by: Dickson, A. G. and Goyet, C., 1994.

Edmond, J. M.: High precision determination of titration of alkalinity and total CO_2 of seawater by potentiometric titration, Deep-Sea Res., 17, 737–750, 1970.

Emery, W. J. and Meincke, J.: Global water masses: summary and review, Ocean. Acta, 9, 383–391, 1986.

Feely, R. A., Sabine, C. L., Key, R. M., and Peng, T. H.: CO_2 survey synthesis results: Estimating the anthropogenic carbon dioxide sink in the Pacific Ocean, U.S. JGOFS News, 9, 1–16, 1999.

Fiedler, P. C. and Talley, L. D.: Hydrography of the eastern tropical Pacific: A review, Progress in Oceanography, 69, 143–180, 2006.

Friis, P.: A review of marine anthropogenic CO_2 definitions: introducing a thermodynamic approach based on observations, Tellus B, 58, 2–15, doi:10.1111/j.1600-0889.2005.00173.x, 2006.

Goyet, C. and Brewer, P. G.: Biochemical properties of the oceanic carbon cycle, in: Modelling Oceanic Climate Interactions, edited by: Willebrand, J. and Anderson, D. L. T., NATO ASI Series, I 11, Springer, Berlin, Heidelberg, 271–297, 1993.

Goyet, C., and Davis, D. L.: Estimation of TCO_2 concentration throughout the water column, Deep-Sea Res. I, 44(5), 859–877, 1997.

Goyet, C., Coatanoan, C., Eischeid, G., Amaoka, T., Okuda, K., Healy, R., and Tsunogai, S.: Spatial variation of total alkalinity in the northern Indian Ocean: a novel approach for the quantification of anthropogenic CO_2 in seawater, J. Mar. Res., 57, 135–163, 1999.

Gruber, N., Sarmiento, J. L., and Stocker, T. F.: An improved method for detecting anthropogenic CO_2 in the oceans, Biogeochem. Cy., 10, 809–837, 1996.

Kessler, W. S.: The circulation of the eastern tropical Pacific: A review, Progress In Oceanography, 69, 181–217, , 2006.

Le Borgne, R., Feely, R. A., and Mackey, D. J.: Carbon fluxes in the equatorial Pacific: a synthesis of the JGOFS programme, Deep Sea Res. Part II, Topical Studies in Oceanography, 49, 2425–2442, 2002.

Lo Monaco C., Goyet, C., Metzl, N., Poisson, A., and Touratier, F.: Distribution and Inventory of Anthropogenic CO_2 in the Southern Ocean: Comparison of three Data-based Methods, J. Geophys. Res., 110, C09S02, doi:10.1029/2004JC002571, 2005.

Longhurst, A. R.: Ecological geography of the sea, Academic Press, San Diego and London, ISBN: 0-12-455558-6, 398 pp., 1998.

Minas, H. J., Minas, M., and Packard, T. T.: Productivity in upwelling areas deduced from hydrographic and chemical fields,

Limnol. Oceanogr., 31, 1182–1206, 1986.

Murray, J. W., Johnson, E., and Garside, C.: A US JGOFS process study in the equatorial Pacific (EqPac): Introduction, Deep Sea Res. Part II, Topical Studies in Oceanography, 42, 275 pp., 1995.

Murray, J. W., Leinen, M. W., Feely, R. A., Toggweiler, J. R., and Wanninkhof, R.: EqPac: A process study in the Central Equatorial Pacific, Oceanography, 5, 134–142, 1992.

Peng, T.-H., Wanninkhof, R., and Feely, R. A.: Increase of anthropogenic CO_2 in the Pacific Ocean over the last two decades, Deep Sea Res. Part II, Topical Studies in Oceanography, 50, 3065–3082, 2003.

Pennington, J. T., Mahoney, K. L., Kuwahara, V. S., Kolber, D. D., Calienes, R., and Chavez, F. P.: Primary production in the eastern tropical Pacific: A review, Progress In Oceanography, 69, 285–317, 2006.

Pérez, F. F., Álvarez, M., and Ríos, A. F.: Improvements on the back-calculation technique for estimating anthropogenic CO_2, Deep-Sea Res. Part I, 49, 859–875, 2002.

Schneider, W., Fuenzalida, R., RodrÍguez-Rubio, E., Garcés-Vargas, J., and Bravo, L.: Characteristics and formation of Eastern South Pacific Intermediate Water, Geophys. Res. Lett., 30(11), 1581, doi:10.1029/2003GL017086, 2003.

Shaffer, G., Salinas, S., Pizarro, O., Vega, A., and Hormazabal, S.: Currents in the deep ocean off Chile (30° S), Deep-Sea Res. Part I, 42, 425–436, 1995.

Shiller, A. M.: Calculating the oceanic CO_2 increase: A need for caution, J. Geophys. Res., 86, 11083–11088, 1981.

Strub, P. T., Mesías, J. M., Montecino, V., Rutllant, J., and Salinas, S.: Coastal ocean circulation off western South America, in: The Sea vol. 11, edited by: Robinson, A. R. and Brink, K. H., J. Wiley and Sons, New York, 11, 273–314, 1998.

Takahashi, T., Feely, R. A., Weiss, R. F., Wanninkhof, R. H., Chipman, D. W., Sutherland, S. C., and Takahashi, T. T.: Global air-sea flux of CO_2: an estimate based on measurements of sea-air pCO_2 difference, Proceedings Of The National Academy Of Sciences Of The United States Of America, 94(16), 8292–8299, 1997.

Tanhua, T., Waugh, D. W., and Wallace, D. W. R.: Use of SF_6 to Estimate Anthropogenic CO_2 in the Upper Ocean, J. Geophys. Res., 113, C04037, doi:10.1029/2007JC004416, 2008.

Tans, P. P., Fung, I. Y., and Takahashi, T.: Observational constraints on the global atmospheric carbon dioxide budget, Science, 247, 1431–1438, 1990.

Tomczak, M. and Gogfrey, J. S.: Regional oceanography: An introduction. Pdf version 1.2, available from: http://www.es.flinders.edu.au/~mattom/regoc/, 2001.

Touratier, F. and Goyet, C.: Definition, properties, and Atlantic Ocean distribution of the new tracer TrOCA, J. Mar. Syst., 46, 169–179, 2004a.

Touratier, F. and Goyet, C.: Applying the new TrOCA approach to assess the distribution of anthropogenic CO_2 in the Atlantic Ocean, J. Mar. Syst., 46, 181–197, 2004b.

Touratier, F., Goyet, C., and Azouzi, L.: CFC-11, $\Delta 14C$, and 3H tracers as a means to assess anthropogenic CO_2 concentrations in the ocean, Tellus, 59B, 318–325, 2007.

Vázquez-Rodríguez, M., Touratier, F., Lo Monaco, C., Waugh, D. W., Padin, X. A., Bellerby, R. G. J., Goyet, C., Metzl, N., Ríos, A. F., and Pérez, F. F.: Anthropogenic carbon in the Atlantic Ocean: Comparison of four data-based calculation meth-

ods. Global Biological Cycle, in press, 2008.

Waugh, D. W., Haine, T. W. N., and Hall, T. M.: Transport times and anthropogenic carbon in the subpolar North Atlantic Ocean, Deep-Sea Res. Part I, 51, 1475–1491, 2004.

Waugh, D. W., Hall, T. M., McNeil, B. I., Key, R., and Matear, R. J.: Anthropogenic CO_2 in the oceans estimated using transit time distributions, Tellus, 58B, 376–389, 2006.

Wyrtki, K.: The oxygen minima in relation to ocean circulation, Deep-Sea Res., 9, 11–23, 1962.

Wyrtki, K.: An estimate of Equatorial Upwelling in the Pacific, American Meteorogical Society, 11, 1205–1214, 1981.

Zenk, W., Siedler, G., Ishida, A., Holfort, J., Kashino, Y., Kuroda, Y., Miyama, T., and Miller, T. J.: Pathways and variability of the Antarctic Intermediate Water in the western equatorial Pacific Ocean, Progress In Oceanography, 67, 245–281, 2005.